JOURNAL OF CATALYSIS 9, 182–194 (1967)

The Effect of Faujasite Cations on Acid Sites

JAMES T. RICHARDSON

From the Esso Research and Engineering Company Baytown Research and Development Division Baytown, Texas

Received May 12, 1967; revised August 24, 1967

The kinetics of cumene cracking have been examined for a series of faujasites ion-exchanged with alkali and alkaline earth elements. Below 525°C the kinetics are zero order with only dealkylation occurring. Above 525°C the radical mechanisms of dehydrogenation and demethylation also take place. Activities for both the carbonium and radical mechanisms increase with increasing polarizing power, *e/r*, of the cation, with the former dominating at higher values of *e/r*. Quinoline is shown to poison the carbonium but not the radical reaction.

A model of the acid site is introduced in which the bond strengths of acidic hydroxyl groups are perturbed by the polarizing effects of neighboring cations.

Addition of 2% Cu to these faujasites produces a synergistic promotion in which the number of active acid sites is increased by a factor of 1000.

INTRODUCTION

A previous paper in this series discussed the ionizing properties of cations in faujasite cages (*1*). It was shown that polynuclear aromatics adsorbed on these zeolites at room temperature transfer an electron to the cation with the concentration of ionized molecules depending on the difference between the ionization energy of the molecule and the surface electron affinity of the cation. Thus, alkali, alkaline earth, and transition metal ions result in an increasing degree of ionization. Furthermore, these elements have a polarizing effect on other cations in the cage. For example, Mg^{2+} with a large polarizing power, *e/r*, acts upon the energy levels of Cu^{2+} to increase the electron affinity and the amount of aromatic ionization.

This paper describes experiments designed to relate these previous results with catalytic properties. Cumene cracking was selected as a test reaction because of its simplicity, extensive earlier use, and the appearance of an unexpected complication which yielded useful information.

EXPERIMENTAL

The catalysts used have been described in the previous paper (*1*). The unit was a modified Perkin-Elmer Micro-Reactor consisting of a 1/4 inch stainless steel reactor with approximately 300 mg of catalyst, together with appropriate valves for sampling the feed and product with a vapor-phase fractometer. Helium was bubbled through a saturator containing purified cumene at a fixed rate, usually 35 cc/min, and then passed through the catalyst bed. Under these conditions the feed rate was approximately 2×10^{-5} moles/min or, for cumene, 0.5 w/w per hr. The catalyst was dried by heating in helium at 400°C for 16 hr, although 2 hr was found to be sufficient. The temperature was then dropped to 200°C and the feed passed over the bed. Thirty minutes to an hour was required to saturate the catalyst. The temperature was raised by intervals up to 600°C. The feed and products were sampled after 30 min at each temperature. Variations on this procedure were made and are indicated where applicable. In some cases quinoline poisoning was carried out by injecting measured amounts of quinoline into the feed stream so that the slug adsorbed on the catalyst bed.

Results and Discussion

1. *Cumene Dealkylation, Dehydrogenation, and Demethylation*

Cumene dealkylation to benzene and propylene has been used widely as a test for the cracking activity of acid catalysts (*2*).

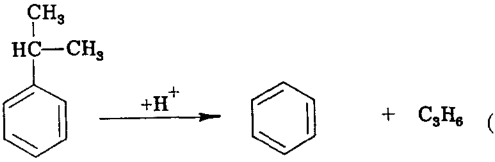
(1)

This reaction is a carbonium ion mechanism and is considered an index to this type of activity. However, free radical cracking of cumene produces styrene and α-methylstyrene (*3*).

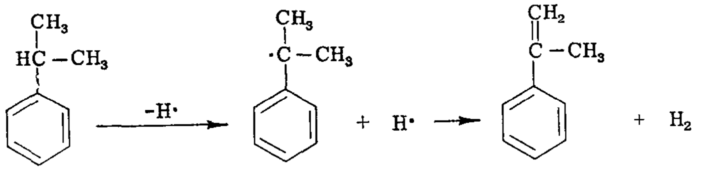
(2)

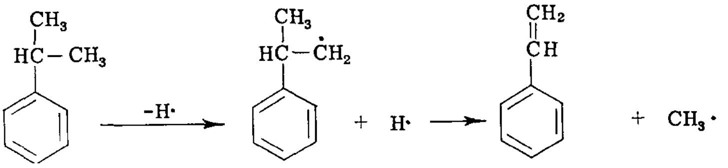
(3)

These reactions have been reported for high-purity alumina catalysts in which the initial step was believed to be dehydrogenation rather than the carbon–carbon bond rupture found in noncatalytic thermal free radical cracking (*4*). The product distribution for cumene cracking may be used as an indication of the relative amounts of carbonium and free radical type activity.

TABLE 1
Cracking of Cumene

Exchange ion	% Aromatic (550°C, 37 cc/min) K	Na	Li	Ba	Sr	Ca	Mg
Cumene	100	100	81	47	30	12	9
Benzene	—	—	—	14	25	59	65
Ethylbenzene	—	—	—	11	13	tr	—
α-Methylstyrene	—	—	19	26	31	29	26

Table 1 shows results for the faujasite ion-exchanged with alkali and alkaline earth ions. Table 2 gives the effect of temperature on two of the catalysts. Below 525°C, only dealkylation occurs. Dehydrogenation to α-methylstyrene starts above 525°C, with demethylation to styrene appearing above 600°C. The appearance of

TABLE 2
Cracking of Cumene—Effect of Temperature

	Ba faujasite (37 cc/min)				Ca faujasite (37 cc/min)					—
Temp. (°C)	400°	500°	550°	600°	400°	450°	500°	550°	600°	650°
Cumene	100	88	47	22	82	69	59	58	31	4
Benzene	—	12	14	24	18	31	41	29	19	21
Ethylbenzene	—	—	11	10	—	—	—	—	6	6
Styrene	—	—	—	3	—	—	—	—	13	32
α-Methylstyrene	—	—	26	38	—	—	—	14	29	33

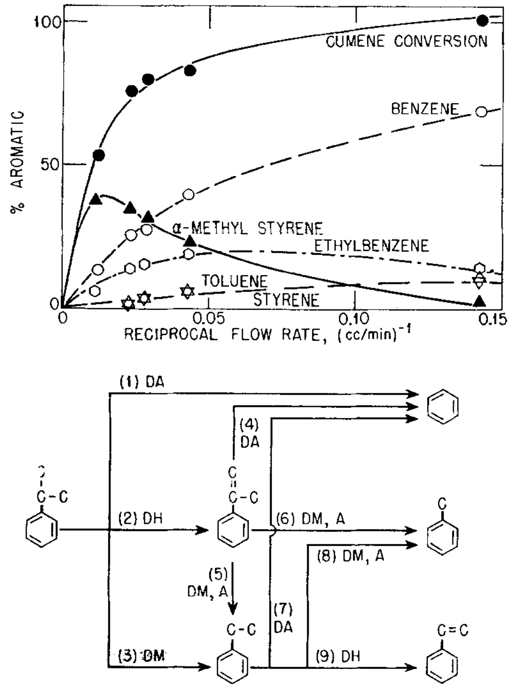

FIG. 1. Product distribution and reaction scheme for cumene cracking.

α-methylstyrene in the prodct also coincides with the presence of ethylene and acetylene in the light gases.

The product distribution is shown in Fig. 1 as a function of contact time (reciprocal flow rate). Ethylbenzene and α-methylstyrene are reaction intermediates which react further as the contact time increases. Product distributions for these two components alone are shown in Figs. 2 and 3. Tests indicated that toluene and styrene did not crack on these catalysts. These data all point to the reaction scheme shown in Fig. 1. Reactions (1), (4), and (7) are clearly carbonium dealkylation processes; reactions (2) and (9) may be classified as radical dehydrogenations, and (3) as a radical demethylation. Reactions (5), (6), and (8) may arise from further demethylation of the intermediates but most likely result from benzene alkylation by reactive $CH_3\cdot$ species. For this reason toluene is regarded as indicative of primary dealkylation activity.

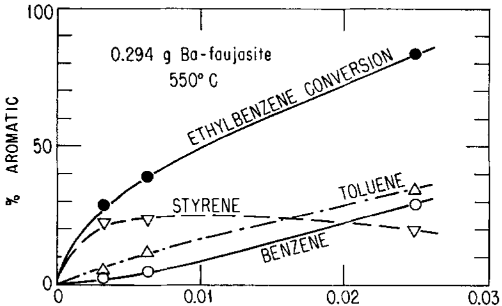

FIG. 2. Ethylbenzene conversion on Ba-faujasite.

The ratio of the concentration of benzene and toluene to the other aromatics may be taken as the relative carbonium to radical activity. Figure 4 shows that this ratio increases with increasing contact time. Comprehensive data of this type are not available for the complete ion-exchanged series; however, for comparative purposes the ratios at one flow rate may be used. These ratios are given in Table 3, and are initial values since poisoning, either by

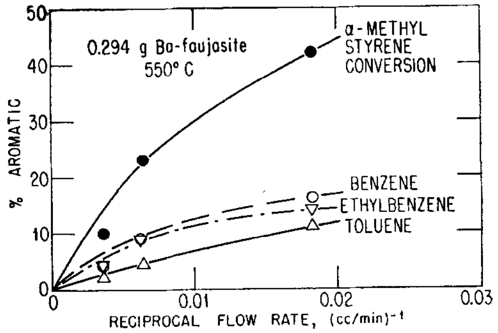

FIG. 3. α-Methylbenzene conversion on Ba-faujasite.

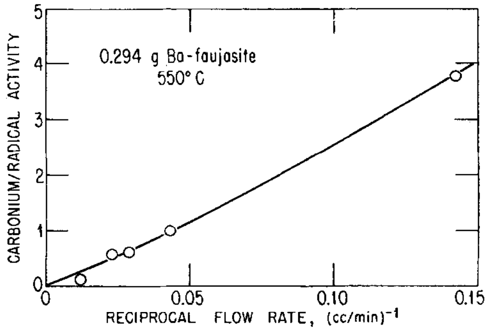

FIG. 4. Rate of carbonium to radical activity versus contact time.

TABLE 3
RATIOS OF CARBONIUM ACTIVITY TO RADICAL ACTIVITY[a]

Ion	C/R
K	0
Na	0
Li	0
Ba	0.43
Sr	0.59
Ca	2.03
Mg	2.50
H	∞

[a] 550°C, 37 cc/min.

Brönsted poisons or coke, decreases the ratio.

When 2% Cu is added to the above samples the activity increases to complete conversion to benzene at 550°C. These results are discussed in greater detail below.

TABLE 4
CUMENE CRACKING

Temp. (°C)	% Cumene conversion (37 cc/min)		
	Cd	Ag	H
200°	0	0	21
250°	—	5	73
300°	6	20	87
400°	91	100	100

Table 4 gives the results for faujasites containing Cd, Ag, and H.

2. *Poisoning of Active Sites*

Table 5 shows a time study on Ag faujasite at 550°C.

At these high levels of conversion the catalyst deactivates rapidly. This is presumably through coke poisoning, since the activity is restored by regeneration with O_2 at 500°C. However, as the dealkylation activity (reflected by the benzene concentration) decreases, the dehydrogenation activity (indicated by the α-methylstyrene) increases. The deactivation finally levels off at about 35% conversion.

These results suggest that coke formation poisons the active dealkylation sites selectively. It was decided to repeat this experiment with a more exact and controlled poison, such as quinoline. Quinoline is a known poison of Brönsted sites through the formation of a $H{-}N^+$ adsorption bond (*5*). It is also an electron donor, such as anthracene, and may form similar charge transfer complexes at the cation site. However, ESR measurements did not reveal any such complexes when quinoline was added to these samples. This was, however, at room temperature. At 550°C this poisoning mechanism is still possible but the proton site deactivation is expected to predominate.

TABLE 5
EFFECT OF COKING ON AG FAUJASITE[a]

Time (hr)	% Conversion	% Benzene	% α-Methyl-styrene
0.75	100	100	0
2.08	82	75	7
2.50	54	24	30
2.83	50	19	31
4.08	36	13	23
4.75	35	12	23
5.33	34	11	23
0.50[b]	100[b]	100[b]	0[b]

[a] 550°C, 38 cc/min.
[b] 18 hr in O_2 at 500°C.

The results, shown in Fig. 5, are similar to those reported by others (*6*, *7*). Small amounts of quinoline were injected into the feed stream and the product sampled 15 min later. It was assumed that all the quinoline was adsorbed on the catalyst bed. The dealkylation activity decreased rapidly until a level of about 45% conversion was reached. At this point, corresponding to one quinoline molecule per faujasite cage, the product was almost completely α-methylstyrene. This indicates that all the dealkyl-

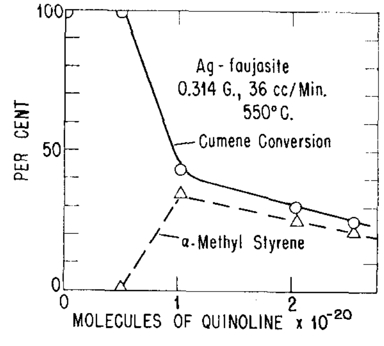

FIG. 5. Quinoline poisoning of Ag-faujasite.

ation sites were deactivated and that only dehydrogenation activity remained. Further poisoning resulted in a decrease in activity but at a much reduced rate.

In another experiment, the poisoning was carried out at lower temperatures where the dehydrogenation does not occur. Figure 6 shows the results. At 300°C the dealkylation sites deactivated rapidly. An increase in temperature up to 325°C resulted in a small increase of activity, but the catalyst continued to deactivate at the some rate.

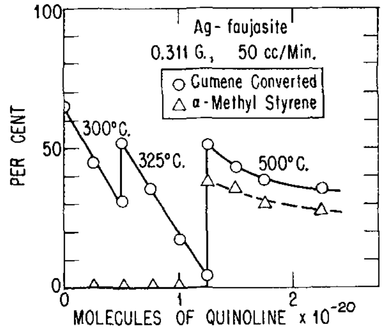

FIG. 6. Quinoline poisoning of Ag-faujasite.

Finally, after the poison level reached about one quinoline molecule per cage, the temperature was raised until at 500°C the dehydrogenation activity commenced. Further poisoning gave a small decrease in activity.

These results confirm that the dealkylation activity is initiated by proton sites which are poisoned selectively by quinoline and coke intermediates. The dehydrogenation sites are not affected by these poisons.

3. *Dealkylation Kinetics*

Figure 7 shows that for H faujasite a plot of dealkylation conversion versus reciprocal flow rate is linear. This indicates a zero order reaction, which is interpreted as the result of strongly adsorbed molecules completely covering available sites and decomposing. Under these conditions, absolute reaction-rate theory gives (*2*)

$$\frac{-dn}{dt} = N_a \frac{kT}{h} \exp\left(-\frac{E}{RT}\right) \quad (1)$$

where —*dn/dt* is the overall rate of cumene disappearance; *k*, the Boltzmann constant; *h*, Planck's constant; *T*, the temperature; *E*, the activation energy; and N_a the number of active sites

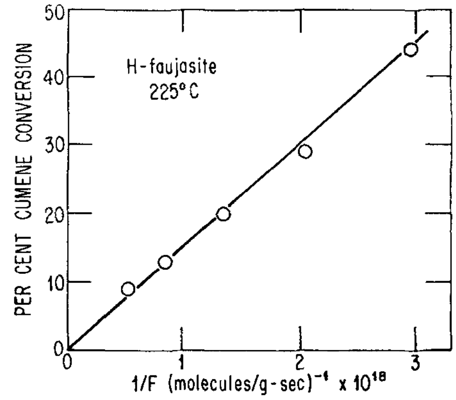

FIG. 7. Zero order kinetics for cumene dealkylation on H-faujasite.

Integrating and expressing results as conversion gives

$$C = \frac{N_i - N_f}{N_i} = \left(N_a \frac{kT}{h}\right) \exp\left(-\frac{E}{RT}\right) \frac{t}{N_i} \quad (2)$$

where N_i and N_f are the initial and final concentrations of cumene.

Furthermore

$$F = N_i/tw$$

where *w* is the weight of catalyst. The slope of *C* versus 1/F (Fig. 7) is a rate constant given by

$$k' = \left(C_A \frac{kT}{h}\right) \exp\left(-\frac{E}{RT}\right) \quad (3)$$

where

$C_A = N_a/w$ = number of active sites per gram

These results are consistent with kinetics reported by others for silica and alumina catalysts (*8*).

4. *Activity of Copper in Faujasite Cages*

Extensive results have been published (*1*) on the properties of various amounts of copper in the faujasite cages. It was found that copper with a large electron affinity easily abstracts electrons from molecules with low ionization energies, but that this ionizing ability is affected by the polarizing power of neighboring cations. In view of this it was important to test the catalytic properties of these samples. Cumene cracking measurements were carried out to examine the effect of (a) temperature of dehydration; (b) concentration of copper; (c) polarizing power of other cations; (d) poisoning by quinoline.

Figure 8 shows the effect of temperature of dehydration on the activity of 2% Cu-Mg faujasite. In this experiment the catalyst was heated in helium at the indicated temperature for 2 hr, then cooled to 300°C, where the activity was measured. The curve shows a steady increase above 300°C, reaching a plateau at 500°C. The leveling of the conversion may be due to completed activation of the sites or to a compensated effect through loss of crystallinity with higher temperatures. Extrapolating the curve to lower temperatures indicates the onset of activity at a dehydration temperature of 200°C. The results of similar measurements on the effect of dehydration temperature on water content and anthracene ionization have been reported (*1*). A comparison of these data with those in Fig. 8 is shown in Fig. 9. The beginning of cumene conversion and anthracene ionization occurs at 200°C. However, ESR spectra show that the Cu^{2+} ions are completely exposed at a level of about 2.5 molecules H_2O per cage. At this point the anthracene spin intensity has reached 85% of its maximum value compared with 47% for the cumene conversion. Exposure of the Cu^{2+} ion is necessary to initiate the reaction but complete activity is not achieved until the H_2O content falls below one per cage.

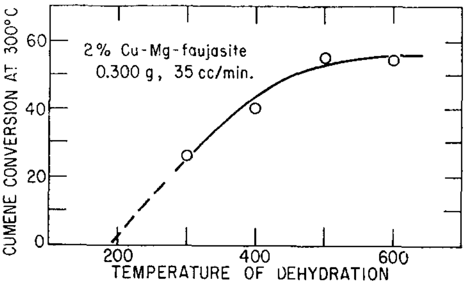

FIG. 8. Cumene conversion versus temperature of dehydration.

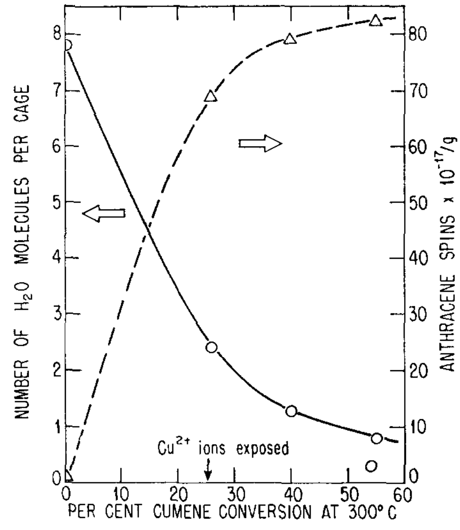

FIG. 9. Effects of dehydration.

A series of samples with increasing copper concentration in Na faujasite was also examined. The results are shown in Fig. 10 with a plot of log k' versus $1/T$. The data show linear relationships and the same activation energy, E, of 28.2 kcal/mole. This compares with 27 kcal/mole previously reported for silica alumina (*2*, *8*) and 30 kcal/mole for Linde Y. Using Eq. (3), the data were extrapolated to give the values of C_A shown in Table 6.

This interpretation relates the increase of activity with an increasing number of adsorbed molecules. It is interesting that the number of such species induced by the copper ions increases from 2 to 14×10^{-8} as the cages fill with copper. This extremely

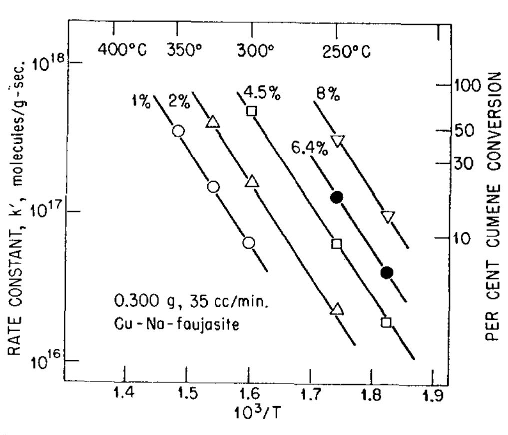

FIG. 10. Arrhenius plots for Cu-faujasite samples.

TABLE 6

C_A VALUES FOR CU-EXCHANGED NA FAUJASITE

Wt % Cu	C_A (sites/g)	Number of Cu^{2+} ions/g
1.0	2.35×10^{13}	9.48×10^{20}
2.0	7.00×10^{13}	1.89×10^{21}
4.5	1.92×10^{14}	4.29×10^{21}
6.4	4.25×10^{14}	6.10×10^{21}
8	1.03×10^{15}	7.53×10^{21}

TABLE 7

C_A VALUES FOR Cu^{2+} IN THE K-MG FAUJASITES

Faujasite	C_A (sites/g)
2% Cu in K faujasite	2.81×10^{12}
2% Cu in Na faujasite	7.00×10^{13}
2% Cu in Li faujasite	1.25×10^{14}
2% Cu in Ca faujasite	7.91×10^{14}
2% Cu in Mg faujasite	5.07×10^{15}
H faujasite	5.75×10^{16}
Mg faujasite	5.20×10^{12}

small number is not unusual in catalysis and is similar to those reported for silica-alumina (*8*).

Figure 11 shows similar data for the series K-Mg faujasite containing 2 wt % Cu^{2+}. The activation energies are all the same and the values of C_A are given in Table 7, together with the values for the faujasite and Mg faujasite.

As the cation changes from K through Mg, the value of C_A increases by a factor of 2,000. This is a remarkable demonstration of the effect of different cations on the catalytic properties of yet another ion. This activity must be due to the copper ion since adding 2% Cu to Mg faujasite increases C_A from 5.20×10^{12} to 5.07×10^{15}—a factor of 1000!

Quinoline poisoning experiments were also made on these samples. Some investigators have used this technique to "titrate" catalysts as a measure of the number of active sites (*6, 7*). This has been done on three of the catalysts. The results, given in Table 8, are similar to those reported above, where dealkylation activity at 550°C only existed above a conversion level of 80%.

TABLE 8

QUINOLINE POISONING OF CU SITES

Catalyst	G (μl)	No. poisoned sites/g
2% Cu-K faujasite	50	9.0×10^{20}
2% Cu-Li faujasite	260	5.28×10^{21}
2% Cu-Mg faujasite	>370	$>7.45 \times 10^{21}$

At a certain quinoline content, *G*, the product was almost all α-methylstyrene, signifying that *G* amount of poison was necessary to destroy the dealkylation sites.

These numbers are in each case a factor of ~10^6 greater than the kinetic expressions

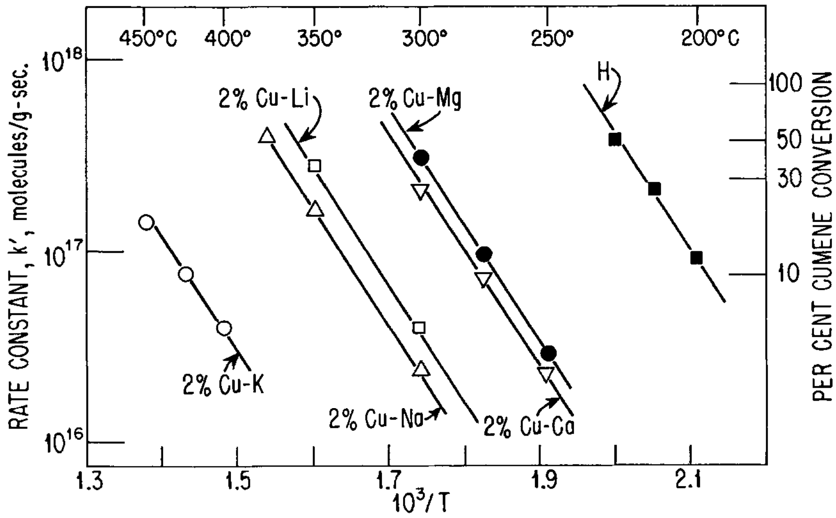

FIG. 11. Arrhenius plots for 2% Cu in K-Mg-faujasite samples.

for C_A. This difference has been reported in the literature for identical poisoning and kinetic measurements on silica-alumina (*2*). Since it is not at all certain that the quinoline was all adsorbed on the catalyst bed, these numbers must be regarded as upper limits only.

Quinoline poisoning experiments have been performed on H faujasite to determine the effect on cumene conversion. The results are summarized in Table 9. The only reaction was dealkylation at all times. Decrease in conversion did not result in α-methylstyrene formation as previously. This indicates that the radical dehydrogenation reaction *does not* take place on H-faujasite and that this activity must be associated with the presence of cations.

TABLE 9

QUINOLINE POISONING OF H FAUJASITE[a]

Quinoline (μl)	Cumene conversion (%)	Benzene conversion (%)
0	100	100
120	100	100
130	91	91
210	67	67
460	43	43
560	31	31
710	15	15

[a] 0.308 g, 35 cc/min., 550°C.

5. *A Model of Acidic Sites in Faujasite*

Results from this laboratory have outlined the oxidative or electron-attracting properties of various cations in the faujasite supercage (*1*), changes in the electron distribution of the Cu—O bonds (*9*), and now the catalytic behavior for carbonium and radical mechanisms. It is worthwhile at this point to examine these data with the objective of elucidating a model for the acidic or catalytic site of the faujasite.

Two main theories for catalytic sites have evolved to date. The "carboniogenic center" theory proposed by Pickert *et al.* is based on the electrostatic field originating from the supercage cation (*10*). Calculations show that this field must be of the order of several volts per angstrom and strong enough to polarize or even fracture hydrocarbons entering the cavity. These polarized species form pseudocarbonium ions with participate in catalytic reactions with other molecules. This elegantly simple theory is supported by activity data similar to that reported above (*10*), by calculations on expected fields with both X and Y type zeolites (*11*), and by infrared measurements which show that CO adsorbs at the cations with a frequency shift that does indeed correlate with the calculated field strength (*12*). The simplicity of this model lends itself to the qualitative understanding and prediction of such cationic effects.

However, the unexplained nature of the pseudocarbonium ion and subsequent reaction steps add unnecessary complications to the theory. The model fails to account for Brönsted acidity which requires the presence of some activated proton or hydroxyl group. There is no reason to believe that the nature of acidity of the crystalline aluminosilicates should be basically different from that of the amorphous materials. Here the necessity for inherent or latent Brönsted protons is well established. The "carboniogenic center" theory does not satisfactorily explain the poisoning of activity by classical Brönsted poisons such as quinoline. Furthermore, the proponents themselves must invoke a different model to explain the catalytic activity of the "decationized" or "dehydroxylated" faujasite-type zeolites (*10*). It would appear then that the electrostatic theory is too simple to explain the catalytic phenomena.

The second theory is based on the Brönsted and Lewis sites present in "acid" and "decationized" zeolites. This model, supported by many investigators (*13–15*), considers the active site to be either a Brönsted site, some hydroxyl modification, or else a dehydroxylated Lewis site capable of inducing Brönsted acidity in adsorbing hydrocarbons. The concentration of these sites would be the greatest in the acid or decationized materials. However, they are to be expected in low concentration in other cationic zeolites. The data in Table 7 show that for the most active catalyst, the H faujasite, one site in every 10,000 cavities is sufficient to explain the catalytic conversions. Hydroxylated and dehydroxylated sites will exist from the very nature of the preparation technique and if only present at impurity levels would be of sufficient concentration to yield measurable results. The other cations affect the number of sites, either by stabilizing their presence or by poisoning, much like conventional amorphous silica-alumina is poisoned by alkali and alkaline earth elements.

This model fails to explain the systematic influence of the cations on the Brönsted sites and also the promotional effects found in the presence of the Cu^{2+} ions. It must therefore be regarded as unsatisfactory in explaining the overall catalytic properties of the cations in the faujasite.

However, some combination of these two theories could result in a generally satisfactory model, a compromise which would embrace the essential features of both while avoiding their inherent difficulties. Such a model was proposed by Hirschler in 1963 but has not been developed or discussed in any further detail (*16*). Hirschler pictured the active sites as hydroxyl groups polarized by the ionic potential of the cations with a resulting dependence on e/r. Although appealing, this solution is not altogether satisfactory since the polarization of an O–H bond in the field of a cation would shift positive charge away from the proton if the cation were acting across the volume of the cavity. This would tend to make the proton less acidic as the ionic potential, e/r. increased.

It is possible to adapt this idea by modifying the nature of the proposed polarization. These concepts are included in the following model.

A cross section of the faujasite cage is shown in Fig. 12. The cations are monovalent in this example and three of them are shown. Also shown are several hydroxyl groups. These hydroxyls are the source of Brönsted acidity. It is well known that OH groups persist and are detectable by infrared methods in zeolite samples heated as high as 500°C (*13, 17, 18*). Figure 9 shows that heating at this temperature leaves one water molecule per cage ($\sim 4 \times 10^{20}$/g). Although most of this water is probably associated with the smaller cavities of the faujasite, these molecules could provide a possible source of OH groups. In addition, OH may originate in the structure itself. Uytterhoeven *et al.* (13) have measured the OH content of the Linde Type Y zeolites and find 0.29×10^{20}, 0.61×10^{20} and 11.2×10^{20} per gram for 500°C treatments of NaY, CaY, and NH_4Y, respectively. These authors conclude that the amount of OH in the NaY corresponds to that required to terminate the crystal faces, that the OH in the NH_4Y (now HY) is associated with the sites left after the NH_3 is removed. Both CaY and NaY contain decationized sites with which OH may associate. The concentration of OH in the HY is 2×10^4 greater than the number of active sites for cumene cracking. For Mg faujasite this factor will be about 3×10^8 (Table 7). Clearly. there must be enough OH in all of these faujasites to provide a sufficient source of acid sites.

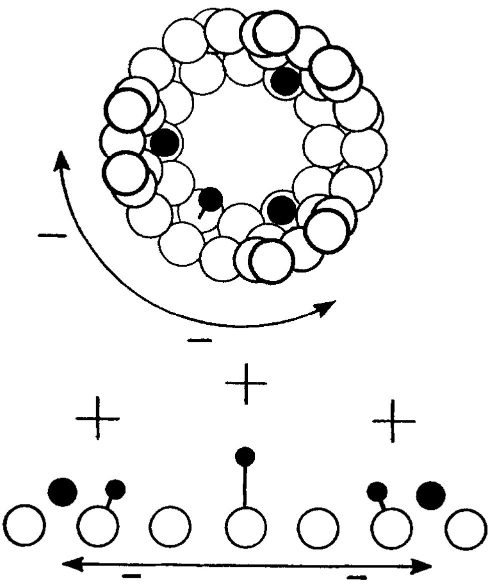

FIG. 12. Cross section of the faujasite cavity.

There are obviously several types of OH groups existing in the supercage, i.e., OH groups attached to different chemical entities and in different environments. Several investigators have studied this problem with infrared spectroscopy with some difference of opinion regarding assignment of the detected bands (*12, 13, 17, 18*). The infrared results are summarized in Table 10.

Carter *et al.*, Habgood, and Uytterhuesen *et al.* agree that the band at 3750 cm^{-1} may be assigned to a Si–O–H vibration. Angell *et al.* concur but believe the species must either be in one of the smaller cavities and thus be inaccessible or else that it is associated with occluded silica-like material. All workers assign the 3695-cm^{-1} band to Al–O–H but they disagree on the exact nature of the band at 3660 cm^{-1}. This band varies from 3590 to 3660 cm^{-1} and shows some dependence on the cation present. Carter *et al.* argue that it is associated with an OH group close to the cation, perhaps even a part of the six-membered oxygen ring. Angell *et al.* assign this band to decationized sites, i.e., Si–O–H with a trigonal Al close by. Its presence in Na and Ca zeolites, they claim, is merely due to the impurity decationized sites present.

TABLE 10
INFRARED BAND ASSIGNMENTS

γ_{aOH} (cm^{-1})	Assignment	Reference
3750	Si–O–H	*13, 17, 18*
	Small cavity Si–O–H or siliceous impurity	*12*
3695	Al–O–H	*12, 13, 17, 18*
3590–3660	Cation-Si–O–H	*17, 18*
	Decat-Si–O–H	*12, 13*

The acid OH group in the model discussed here may be one or all of these. It is unlikely to be an OH directly associated with the cation since the data in Fig. 9 show that the Cu^{2+} ion in 2% Cu-Mg faujasite must be dehydrated or exposed before either anthracene ionization or cumene cracking takes place. The presence of OH groups attached to different chemical environments provides the energy heterogeneity of active sites known to exist on many surfaces.

Granted the existence of acid OH groups in at least a sufficient number of faujasite cages, how are these perturbed by the cations in order to show the observed dependence? Direct polarization across the cavity has been ruled out since this would result in opposite effects. However, the cations may exert an influence via the intervening crystal structure.

The presence of the aluminum in the faujasite structure requires a balancing negative charge associated with each aluminum-oxygen tetrahedron. It is not necessary to consider these charges as immobilized. Indeed, the faujasite is a solid and although technically an insulator may be interpreted with electronic band theory. The intrinsic energy band gap is no doubt large (of the order of 10 eV) but each negative charge constitutes a donor level. The levels have a large enough concentration (2×10^{21}/cc) and have sufficiently large wave functions that conduction or charge motion may occur within a broadened impurity band (*19*). The cations now become positively charged surface defects that will attract negative charge, so that the negative charge distribution tends to concentrate in the vicinity of the cations. The greater the electron-attracting properties of the cation, the greater the concentration of electrons in its neighborhood. As the negative charge distribution is pulled toward the cation, the electron cloud of the OH band will be pulled toward the oxygen atom. The larger the electron affinity of the cation, the closer this cloud moves toward the oxygen and the more positive will be the hydrogen atom (i.e., the site will be more acidic). This is exactly the same mechanism that raises the $d_{x^2-y^2}$ level of the Cu^{2+} ion as neighboring cations change from K^{+} through Mg^{2+} (*9*).

There are no direct measurements of acidity available for these samples. The usual indicators are so large that interpretation becomes difficult. The application of the recently developed pyridine adsorption infrared techniques has not been applied to cationic faujasite series (*20*). The correlation of OH vibration frequencies with acidity (*21, 22*) and electronegativity of constituents (*23*) has been attempted. The

---

* *Note added in proof:* See, however, Eberly, P. E., 154th Meeting, American Chemical Society, Chicago, September 1967, Abstract I42.

only useful observations applicable here are that the OH frequency increases as the electronegativity of the attached atom decreases, and the OH frequency decreases as the acidity increases. In this last case, a study of OH groups on carboxylic acids revealed an increase of 100 cm^{-1} as the pK$_a$ changed from 0.3 to 10.3 (*23*). This implies that the reported shifts associated with the band at 3590–3660 cm^{-1} may reflect large variations in acidity. This supports the findings of Angell *et al.* whose results for cations of increasing acidic reactivity are shown in Table 11.

TABLE 11

γ_{OH} VALUES OF LINDE Y ZEOLITES WITH INCREASINGLY ACIDIC CATIONS

Cation	γ_{OH}
NaY	3652
BaY	3647
CaY	3645
MgY	3643
Decat Y	3636

If the assignments of Angell *et al.* are accepted, the band at 3750 cm^{-1} is Si–O–H that is not associated with the structure of the cavity. The band at 3695 cm^{-1} is Al–O–H and is similar to that found in Al_2O_3. It is not unreasonable to assume an acid strength of pK$_a$ = +4.95 for Al_2O_3 (*16*). With this value as a starting point, the data of Goulden (*22*) may be extrapolated and the observed differences in OH vibrations for various pK$_a$ values used to estimate the equivalent pK$_a$ for the bands at 3636–3652 cm^{-1}. On this basis a speculative picture of the acid site distribution may be assembled. This is shown in Fig. 13.

There are two centers of acid strength distribution, each corresponding to the respective Al–O–H and Si–O–H (cation) bands. The full line in Fig. 13 applies to NaY. The sites Al–O–H are weakly acidic and do not contribute to the catalytic acidity. The sites Si–O–H (cation), however, are more acidic. This double peak distribution would give similar experimental results to those observed by Hirschler for a titrated CaX sample (*16*). The distribu-

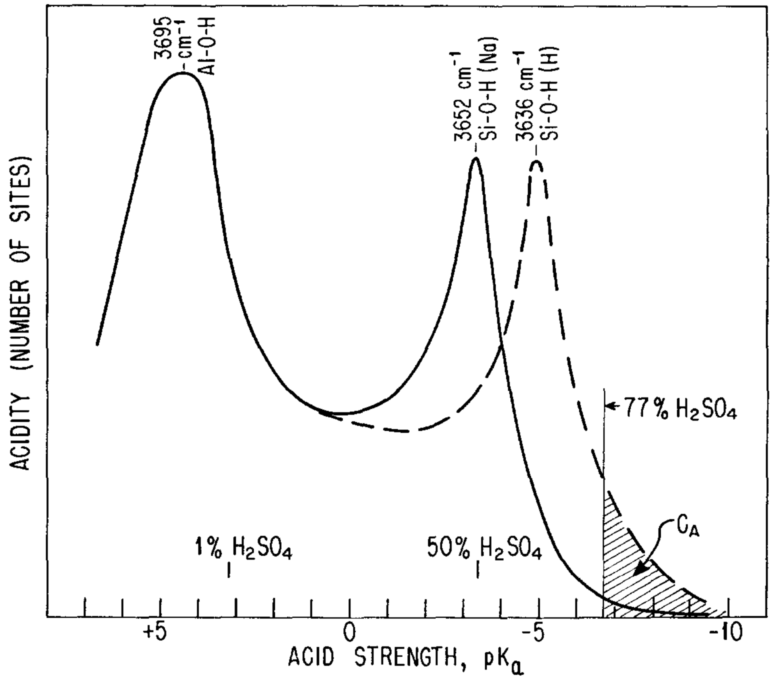

FIG. 13. Proposed acid strength distribution for faujasites.

tion of the Si–O–H (cation) peak drops sharply so that only a small number of sites are strongly acid. If, as claimed by Hirschler (*16*), 77% H_2SO_4 strength is required for cumene cracking, then only those sites in that portion of the distribution will be active.

As the polarizing power (e/r) of the cation increases, the Al–O–H (cation) peak shifts to higher acidities. The curve for H-Y Linde is shown as the dotted line in Fig. 13. The change in γ_{OH} of only 16 cm^{-1} corresponds to a shift in peak position from $pK_a = -3.3$ to $pK_a = -4.9$. The result is to move the tail of the distribution to higher acid strengths, so that more sites now lie above the 77% H_2SO_4 limit. The increase in the number of effective sites is reflected by the increase in C_A observed in the kinetic parameters above. The actual ratio of effective sites is much higher for the two catalysts than shown in Fig. 13, since the shapes of the distribution tails have been arbitrarily chosen to illustrate the principle rather than account for the quantitative aspects.

This model is rather speculative and only semiquantitative. It has, however, been assembled from a collection of experimental data, both from this laboratory and elsewhere. It fits the facts in a consistent manner and it serves as a useful aid in the understanding of zeolite acidic phenomena.

6. *Radical Sites in Faujasite*

The acid OH groups in the faujasite cavity are responsible for the carbonium ion activity observed in the cumene cracking. The radical dehydrogenation reactions must involve different sites since these are not affected by Brönsted poisons such as quinoline.

The most obvious catalytic sites are the the cations themselves. Their ability to generate radical cations in aromatics is established (*1*). The radical dehydrogenation activity seems to increase with the electron affinity of the cation, but this has not been definitely established.

If the dehydrogenation activity does indeed correlate with the aromatic ionizing abilities of these faujasites, it is not clear at this point why there is no dehydrogenation with the acid faujasite.

7. *Promotional Effects with Copper*

It has been discussed above how the addition of 2% Cu to Mg faujasite increases C_A from 5.20×10^{12} to 5.07×10^{15} and how changing the cation from K to Mg results in C_A's from 2.81×10^{12} to 5.07×10^{15}. Similar effects for anthracene radical-cation formation have been demonstrated (*1*). The explanation consistent with the above model is that the increased ionic potential lowers the electronic energy levels of the Cu^{2+} *d*-electrons. This is similar to the behavior of the hydrogen atom in an electric field. The result of this energy level lowering is an increase in electron affinity with subsequent increase of the number of effective acid sites. An increased splitting of the *d* levels is superimposed upon this overall decrease (*1, 9*).

Extending the obvious conclusions of this phenomenon, the most pronounced promotional effects may be expected for cations with large electron affinities under the influence of other cations with large values of e/r. This prediction has been confirmed in a system to be discussed in a subsequent publication.

The possibility of reduction of the Cu ions to the metal by the feed, even in this low a concentration, should be considered. This process would leave protons behind in the supercage, thus creating a type of H-faujasite, which would increase the number of active sites. However, it is difficult to understand how this process would give the wide variation in C_A as the cation changes from Na to Mg. Since the samples all contain the same amount of Cu, the same reduction properties would be expected, resulting in the same activity for all the samples. Furthermore, *in situ* ESR measurements (using a special high-temperature device to be described elsewhere) carried out under reaction conditions, failed to show any change in the hyperfine structure so characteristic of Cu^{2+} in the faujasite environment. The role of reduction in the above effects is not considered to be very important.

CONCLUSIONS

A model for the acid sites in faujasite-type zeolites has been proposed. This model fulfills the experimental requirements and overcomes the objections to previous models. The results for cumene cracking and catalyst poisoning show two types of active sites, one associated with the acidic OH groups and the other with the cations. The kinetics of cumene dealkylation and dehydrogenation over faujasites with various cations are consistent with the model. The model also explains previous results obtained by others with other techniques and serves a useful purpose in the further understanding and prediction of acid catalysis.

ACKNOWLEDGMENTS

The author acknowledges the assistance of Mr. S. S. Toups, who carried out many of the experimental operations, and the helpful discussions of Dr. F. H. Field, Dr. R. A. Velapoldi, and Professor F. A. Matsen

REFERENCES

1. RICHARDSON, J. T., *J. Catalysis* **9**, 172 (1967) (this issue).
2. PRATER, C. D., AND LAGO, R. M., *Advan. Catalysis,* **8**, 293 (1956).
3. LEIGH, C. H., AND SZWARC, M., *J. Chem. Phys.* **20**, 844 (1952).
4. TUNG, S. E., AND MCININCH, E., *J. Catalysis* **4**, 586 (1965).
5. MILLS, G. A., BOEDEKER, E. R., AND OBLAD, A. G. *J. Am. Chem. Soc.* **72**, 1554 (1950).
6. BORESKOVA, E. G., TOPCHIEVA, K. V., AND PIGUZOVA, L. I. *Kinetika; Kataliz* **5**, 903 (1964).
7. TURKEVICH, J., NOZAKI, F., AND STAMIRES, D., *Proc. Intern. Congr. Catalysis, 3rd, Amsterdam, 1964* **1**, 586 (Wiley, New York, 1965).
8. HORTON, W. B., AND MAATMAN, R., *J. Catalysis* **3**, 113 (1964).
9. RICHARDSON, J. T., *J. Catalysis* **9**, 178 (1967) (preceding paper).
10. PICKERT, P. E., RABO, J. A., DEMPSEY, E., AND SHOMAKER, V., *Proc. Intern. Congr. Catalysis, 3rd, Amsterdam, 1964* **2**, 1264. (Wiley, New York, 1965).
11. RABO, J. A., ANGELL, C. L., KASAI, P. H., AND SCHOMAKER, V., *Discussions Faraday Soc.* **41**, 328 (1966).
12. ANGELL, C. L., AND SCHAFFER, P. C., *J. Phys. Chem.* **70**, 1413 (1966).
13. UYTTERHOEVEN, J. B., CHRISTNER, L. G., AND HALL, W. K., *J. Phys. Chem.* **69**, 2117 (1963).
14. STAMIRES, D. N., AND TURKEVICH, J., *J. Am. Chem. Soc.* **86**, 757 (1964).
15. HIRSCHLER, A. E., *J. Catalysis* **6**, 1 (1966).
16. HIRSCHLER, A. E., *J. Catalysis* **2**, 428 (1963).
17. CARTER, J. L. LUCCHESI, P. J., AND YATES, D. J. C., *J. Phys. Chem.* **68**, 1385 (1964).
18. HABGOOD, H. W., *J. Phys. Chem.* **69**, 1764 (1965).
19. HANNAY, N. B., ED., "Semiconductors." Reinhold., New York, 1959.
20. BASILA, M. R., KANTNER, T. R., AND RHEE, K. H., *J. Phys. Chem.* **68**, 3197 (1964).
21. BORISOVA, M. S., DZIS'KO, V. A., IGNAT'EVA, L. A., AND TIMOFEEVA, L. N., *Kinetika i Kataliz* **4**, 461 (1963).
22. GOULDEN, J. D. S., *Spectrochim Acta* **6**, 129 (1954).
23. WEST, R., AND BANEY, R. H., *J. Phys. Chem.* **64**, 822 (1964).